STATISTICAL DESCRIPTION OF NONLINEAR WAVE FIELDS

V. E. Zakharov and V. S. L'vov

UDC 538.56:519.25

A description of the Wyld diagram technique is given in the language of canonical variables for classical wave fields. It is shown that this technique describes thermodynamic equilibrium in particular; it may also be used to validate the applicability of the kinetic equation for waves. The problem of a turbulent sealing is discussed, together with its relationship to the power-law spectra of weak turbulence.

INTRODUCTION

Various physical situations (plasma turbulence, the passage of high-power laser pulses through matter, parametric excitation of spin waves in ferromagnetic materials, etc.) necessitate the statistical description of nonlinear wave fields under conditions that are in no way near thermodynamic equilibrium. For elementary cases (low-level nonlinearity and certain restrictions on the wave-dispersion law), such a description may be given in the language of kinetic equations. The corresponding theory is usually referred to as the theory of weak turbulence. Attempts to go beyond the framework of weak turbulence require the use of diagram techniques.

There are several types of diagram techniques suitable for the description of nonequilibrium systems (see [1, 2], for example). It is most natural to use the Wyld technique [1] for classical problems; it was constructed in 1961 for the example of a hydrodynamic-type equation and served as the basis for numerous studies on the turbulence of an incompressible fluid (see [3, 4], for example). Although the wave-field equations encountered in physical problems, written in "natural" variables (velocity, pressure, the electromagnetic field, etc.), are usually not Hamiltonian equations, they ordinarily possess a latent Hamiltonian structure (see [5]). By bringing out this structure (introducing canonical variables), it is possible to make a substantial simplification in the solution of fundamental nonlinear problems. Our aim here is to describe the Wyld diagram technique in the language of canonical equations for classical wave fields (sec. 1).

By using canonical variables, it is possible to show that the Wyld technique describes thermodynamic equilibrium in particular (sec. 2). Although this fact is natural, no proof has so far been given in the "ordinary" Wyld technique. Our proof makes use of the symmetry properties of "bare" vertices, which hold only for canonical variables, and it is formulated as a "fluctuation-dissociation theorem" (i.e., it asserts the compatibility of the diagram equations with the thermodynamic relationship between the spectral density and the Green's function). In this way, we obtain a purely classical proof of the fluctuation-dissociation theorem.

Using the diagram technique, it is easy to derive the familiar kinetic equations for waves and to obtain corrections for them in the regular manner. In particular, this enables us (sec. 3) to validate the limits of applicability of the kinetic equation (i.e., the weak turbulence approximation): the wave damping γ_k characterizing the level of system nonlinearity must be less than $\Delta k(\partial\omega_k/\partial k)$ and less than $(\partial^2\omega_k/\partial k^2)(\Delta k)^2$, where Δk is the characteristic width of a wave packet.

Institute of Theoretical Physics, Academy of Sciences of the USSR. Translated from Izvestiya Vysshikh Uchebnykh Zavedenii, Radiofizika, Vol. 18, No. 10, pp. 1470-1487, October, 1975. Original article submitted December 16, 1974.

The next topic that is conveniently treated in the canonical technique is the question of turbulent scaling. The success of scale-invariance methods in the theory of phase transitions and the formal similarity of the phase-transition and strong-turbulence problems lead naturally to the concept of transferring the scaling methods developed in recent years to the case of turbulence.

We might hope that these methods will lead to future progress in the central problem of strong-turbulence theory, the problem of the Kolmogorov spectrum. In this study (sec. 4), we have made just the first step in this direction: we show that in elementary cases the additional scaling index which appears owing to departure from thermodynamic equilibrium may be found by means of a conformal frequency transformation analogous to the transformation of the kinetic equation for waves that permits us to find the power-law spectra of weak turbulence.

1. DIAGRAM TECHNIQUE

We consider a wave field that in a linear approximation possesses a dispersion law ω_k described by the complex amplitude a_k and having the Hamiltonian

$$H = \int \omega_k a_k a_k^* d\mathbf{k} + H_{int}. \tag{1}$$

We introduce the notation a_k, $a_k^* = a_k^s$ (s = ±1). Initially assuming the interaction Hamiltonian to be cubic in a_k^s, we write it in the form

$$H_{int} = \frac{1}{3!} \int \sum_{s,s',s''} V_{kk'k''}^{ss's''} a_k^s a_{k'}^{s'} a_{k''}^{s''} \delta(s\mathbf{k} + s'\mathbf{k}' + s''\mathbf{k}'') d\mathbf{k}\, d\mathbf{k}'\, d\mathbf{k}''. \tag{2}$$

Since the Hamiltonian is real, we have

$$V_{k\ k'\ k''}^{-s,\ -s',\ -s''} = \left(V_{kk'k''}^{ss's''}\right)^* . \tag{3}$$

Moreover, the coefficients V possess evident "permutation symmetry":

$$V_{kk'k''}^{ss's''} = V_{k'kk''}^{s'ss''} = V_{kk''k'}^{ss''s'} . \tag{4}$$

The equations of the wave field have the form

$$is \frac{\partial a_k^s}{\partial t} = \frac{\delta H}{\delta a_k^{-s}} - is\gamma_k a_k^s + f_k. \tag{5}$$

In this equation we have formally included the wave damping γ_k and the external forces f_k describing the weak interaction of the wave field with the "environment" (the thermostat). We assume the external force $f_k(t)$ to be random with a Gaussian distribution. Assuming

$$a_k^s(t) = \int_{-\infty}^{\infty} a_{k\omega}^s e^{-is\omega t} d\omega \tag{6}$$

and introducing the four-dimensional notation $q = \{\mathbf{k}, \omega\}$, we obtain

$$a_q^s = G_{0q}^s \left[\int dq' dq'' \sum_{s's''} \left(\frac{1}{2} V_{kk'k''}^{-s,\, s's''} a_{q'}^{s'} a_{q''}^{s''} \delta(-sq + s'q' + s''q'') + f_q^s \right) \right]. \tag{7}$$

Here G_{0q}^s is the bare Green's function,

$$G_{0q}^s = \frac{1}{\omega - \omega_k + is\gamma_k}. \tag{8}$$

We consider the formal solution of (7) in the form of a series in powers of f_q:

$$a_q^s = a_{0q}^s + a_{1q}^s + a_{2q}^s + \dots,$$

$$a_{0q}^s = G_{0q}^s f_q^s,$$

$$a_{1q}^s = G_{0q}^s \int dq' dq'' \sum_{s',s''} \frac{1}{2} V_{kk'k''}^{-s,\, s's''} G_{0q'}^{s'} G_{0q''}^{s''} \delta(-sq + s'q' + s''q'') f_{q'}^{s'} f_{q''}^{s''}, \tag{9}$$

$$a_{2q}^s = G_{0q}^s \int dq' dq'' \sum_{s's''} \frac{1}{2} V_{kk'k''}^{-s,\, s's''} \left(a_{0q'}^{s'} a_{1q''}^{s''} + a_{0q''}^{s''} a_{1q'}^{s'} \right) \delta(-sq + s'q' + s''q'').$$

Using the graphical definitions

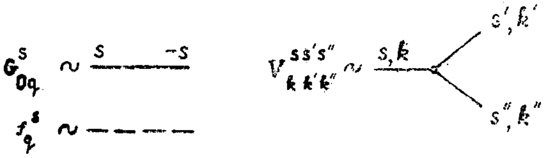

(9a)

we may place each term of the above series into juxtaposition with a diagram.

Each diagram of the series for a_q constitutes a "tree" branching at vertices V whose top terminates in dashed random-force lines. The vertices $V^{ss's''}_{kk'k''}$ must be matched to $\delta(sk + s'k' + s''k'')$, with summation being carried out over all s and integration over all q of the inner lines. The diagrams for a^s_{nq} contain all topologically different trees with n vertices V; the numerical coefficient of each such tree is 1/2. The diagrams corresponding to (10) are

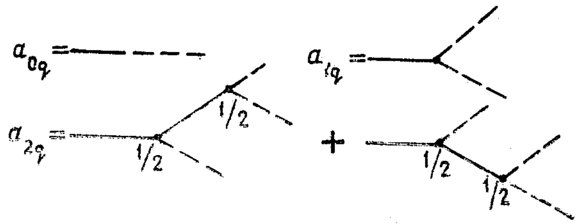

(10)

It is not difficult to see that the analytical expressions corresponding to trees going over into one another when a portion of the tree is rotated about some vertex will coincide. The first example of this sort is two trees for a_{2q}. We henceforth assume such trees to be topologically equivalent, assuming that there is a number of them such that we retain the discriminating factor 1/2 only at "symmetric" vertices (i.e., vertices from which a rotationally symmetric tree "grows"). As a result, the entire diagram acquires a discriminating factor 1/p, where p is the number of elements in its symmetry group, including the identity element. For trees of order two and three, this is represented as

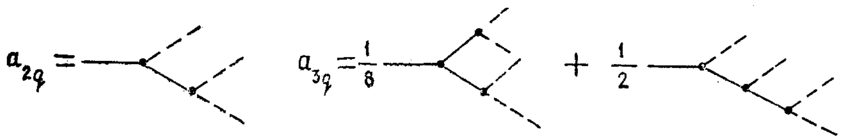

(11)

This possibility of reducing the number of topologically different diagrams is associated in principle with the classical nature of the wave field, which is reflected in the commutativity of the quantities f^s_q. We further note that one of the end points of the tree (its root) is isolated: of the three lines meeting at each vertex, one runs "to the root" and the others "away from the root." As we see from (9), on the line running "to the root" there is a change in the sign of the index s for the vertex.

Let us now calculate the following paired averages: the spectral density n_q and Green's function G_q, the linear response of the system to an external force:

$$\langle a^s_q a^{s'}_{q'} \rangle = n^s_q \delta(q-q') \Delta(s-s'), \qquad n^s_q = n^{-s}_q,$$
$$G^s_q \delta(q-q') = \frac{\langle a^s_q f^{-s'}_{q'} \rangle}{\langle f^s_q f^{-s}_{q'} \rangle} = \left\langle \frac{\delta a^s_q}{\delta f^s_{q'}} \right\rangle. \tag{12}$$

To compute the averages, we make use of the Gaussian nature of the external force f_q and assume that there are no correlators from the product of an odd number of f_q while assuming that the correlators from even products are divided into the sums of products of paired correlators:

$$\langle f^s_q f^{-s}_{q'} \rangle = F^s_q \delta(q-q'), \qquad F^s_q = F^{-s}_q. \tag{13}$$

This partitioning is graphically illustrated by paired "scaling" of the outer branches of the trees. In calculating the average we perform scaling for two trees, which we represent as image reflections from a vertical line. Here for vertices and lines to the right of the tree line all indices s must change sign. To calculate the average for G_q^s, we carry out scaling within one tree with each of its outer branches fixed successively. Carrying out summation of the reduced graphs we arrive at a system of Dyson equations for n_q^s and G_q^s: $G_q = G_{oq}\,[1 + \Sigma_q G_q]$, $n_q = |G_q|^2 \Phi_q$; graphically,

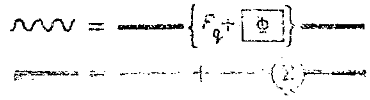

(14)

Here a heavy wavy line indicates n_q, and a heavy straight line indicates G_q:

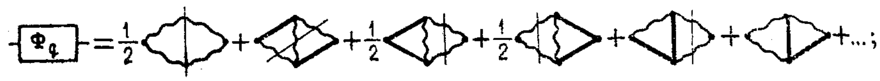

(15)

(16)

The graphs in the series (15) and (16) contain no weakly connected parts separated by two lines. The graphs for Φ_q have two equivalent end points ("roots" of the joined trees); the graphs for Σ_q have differing end points (input and output) corresponding to the "root" of the tree and a fixed branch.

Let us enumerate the topological properties of the graphs for Σ_q and Φ_q that are important for the ensuing discussion:

1. In the diagrams for Φ_q (for Σ_q) from each vertex we may proceed only along G_q' lines toward the input or (and) output in unique fashion. Thus, there are no vertices with three n_q' lines and no closed loops along G_q' lines.

2. In each graph for Σ_q, there exist a unique path connecting the input and output along G_q' lines — the "spine" of the graph. The remaining G_q' lines of the graphs may be referred to as edges.

3. The Φ_q graphs contain a "principal cut" for which they may be uniquely dissected into two parts along n_q' lines only. We shall refer to these n_q' lines as "principal".

4. Clearly, by successively replacing principal n_q' lines by G_q' lines in the graphs for Φ_q, we shall enumerate all topological structures of the graphs for Σ_q.

Let us now indicate the rules for calculating the coefficients of the graphs for Σ_q and Φ_q for a given topological structure:

5. All topologically different graphs for Σ_q have an identical numerical coefficient equalling unity.

6. Topologically different graphs for Φ_q have the coefficient 1/2 if they are symmetric with respect to the line connecting the input and output [for example, the first, third, and fourth graphs in (15)] and the coefficient 1 otherwise.

These rules follow from the fact that in "splicing" of lines running from a symmetric vertex it is possible to double the number of splices by carrying out a rotation at this vertex. This doubling compensates for the factor 1/2 introduced by the symmetric vertex. An exception is represented by the case in which splicing of two symmetric trees preserves a single graph symmetry (with respect to rotation along the end points of the graph).

Let us now define the procedure for graph multiplication. In graphs for Φ_q, we successively isolate each of the fundamental n_q' lines (for example, marking the isolated line by a cross), while in the graphs for Σ_q we successively isolate (also by a cross) each line of the spine. The fundamental structural property of the graphs follows from 1-6:

7. There is a one-to-one relationship between the "multiplied" graphs for Φ_q and Σ_q (including the numerical coefficients). This correspondence is realized by replacing wavy marked lines by straight lines and vice versa.

Let us discuss the rules for reading the graphs. To each graph for Σ_q or Φ_q having n lines there correspond 2^m terms corresponding to different ways of choosing the signs for the indices s_1, s_2, ... It is convenient to represent this choice graphically, assigning a direction to the $G_q^{s'}$ and $n_q^{s'}$ lines. On the graphs for Σ_q and the left side of graphs for Φ_q the functions G_q, n_q should be assigned an arrow "away from the input," while the complex-conjugate functions G_q^* and n_q^* should be assigned an arrow running "to the input." On the part of the graph of Φ_q situated to the right of the principal section the functions $G_{q'}$ and $n_{q'}$ are assigned an arrow "from the output," while $G_{q'}^*$ and $n_{q'}^*$ are assigned an arrow "to the output." With the directions of the arrows chosen in this manner:

8. The delta functions are so arranged at the vertices that the sum of the four-momenta arriving at the vertex equals the sum of those leaving. In any cut of the Σ_q and Φ_q graphs that separates the input from the output, the algebraic sum of all momenta of the lines is q.

Let us show that:

9. In writing the analytical expressions for Σ_q in the product of all vertices and functions $G_{q'}$, only the real part should be left in the edges. As an example, the graph *a*)

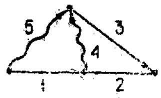

a

corresponds to the expression

$$\int dq_1 \ldots dq_5 G_{q_1} G_{q_2} \mathrm{Re}\left\{ V_{k15}^{-++} V_{124}^{-++} V_{23k}^{--+} V_{345}^{+--} G_{q_3}^* n_{q_4} n_{q_5} \right\} \times$$
$$\times \delta(q - q_1 - q_5)\, \delta(q_1 - q_2 - q_4)\, \delta(q_5 + q_4 - q_3)\, \delta(q_2 + q_3 - q).$$

For the proof we must consider, in addition to the given graph [for example, *a*)], a graph [b) for this case]

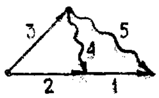

b ,

obtained from its image reflection and complex-conjugate (it corresponds to a change in the directions of all arrows). As a result, the two graphs exhibit coincidence of all delta functions and directions of arrows in the spines; the arrows in the edges change direction [compare *a*) and b)]. Next, in accordance with property 5, we must allow for the fact that both graphs occur in the expression for Σ_q with the same coefficients (equal to unity).

Similarly, considering image-symmetric graphs it is easy to see that:

10. For any graph, only its real part occurs in the analytic expression for Φ_q.

Let us now see how the diagrams for Im Σ_q look. To do this, we make use of an identity holding for an arbitrary set of N complex numbers α_n:

$$\mathrm{Im}(\alpha_1 \ldots \alpha_N) = \mathrm{Im}(\alpha_1 \alpha_2^* \ldots \alpha_N^*) + \alpha_1 \mathrm{Im}(\alpha_2 \alpha_3^* \ldots \alpha_N^*) + \ldots + \alpha_1 \alpha_2 \ldots \alpha_{N-1} \mathrm{Im}\, \alpha_N.$$

Multiplying this identity by an arbitrary complex number β and calculating the real part, we have

$$\mathrm{Re}\,\beta\, \mathrm{Im}(\alpha_1 \ldots \alpha_N) = \mathrm{Im}\,\alpha_1 \mathrm{Re}(\beta \alpha_2^* \ldots \alpha_N^*) + \ldots + \mathrm{Im}\,\alpha_N \mathrm{Re}(\beta \alpha_1 \ldots \alpha_{N-1}). \tag{17}$$

Let us now consider a graph for Σ_q having N lines in the spine. We let β represent the contribution made by the graph edges and let α_n represent the G-functions of the spine. By virtue of rule 10, only the real part of β makes a contribution to the graph. Evaluating Im Σ_q and using (17), we arrive at the following result:

11. To calculate Im Σ_q it is necessary to multiply each graph for Σ_q (using a class to successively mark each of the lines of the spine), replace each labeled G-function by its imaginary part, replace all G-functions of the spine that are located to the right of a labeled line by the complex-conjugates, and remove the real part from each graph. Rule 11 permits direct calculation of Im Σ_q. Cutkosky [6] has described a similar method for calculating imaginary parts in Feynman diagrams for quantum electrodynamics.

For a whole series of interesting physical situations (fluid dynamics of an incompressible fluid, of a cold plasma, etc.), the basic contribution to nonlinearity is made by the interaction of four waves. Writing the Hamiltonian H_{int} as

$$H_{\text{int}} = \frac{1}{4!} \sum_{s_1 s_2 s_3 s_4} V^{s_1 s_2 s_3 s_4}_{k_1 k_2 k_3 k_4} a^{s_1}_{k_1} a^{s_2}_{k_2} a^{s_3}_{k_3} a^{s_4}_{k_4} \times \delta(s_1 \mathbf{k}_1 + s_2 \mathbf{k}_2 + s_3 \mathbf{k}_3 + s_4 \mathbf{k}_4)\, d\mathbf{k}_1\, d\mathbf{k}_2 d\mathbf{k}_3 d\mathbf{k}_4, \tag{18}$$

we may proceed in like manner to formulate a diagram technique and go over to the Dyson equations (14); here for the compact parts of Φ and Σ, we obtain the series


(19)

in place of (15).

All graphs' properties, reading rules, etc., remain as before, except that it is necessary to generalize rules 5 and 6 pertaining to the numerical coefficient on the graphs in the following manner: to each graph there corresponds a discriminating factor 1/p, where p is the number of elements in the symmetry group of the graph, including the identical element.

2. FLUCTUATION-DISSIPATION THEOREM

Let us now show that the equations that we have constructed for n^s_q and G^s_q will in particular describe the thermodynamic equilibrium of a wave field. Calculating the imaginary part of the Dyson equation (14), we obtain

$$\operatorname{Im} G_q = |G_q|^2 \left(\frac{\operatorname{Im} G_{0q}}{|G_{0q}|^2} + \operatorname{Im} \Sigma_q \right). \tag{20}$$

We shall seek a solution of (14) in the form of

$$n^s_q = \frac{T}{(p \cdot q)} \operatorname{Im} G^s_q. \tag{21}$$

Here T is the temperature of the thermostat, and $p = \{\mathbf{V}, 1\}$ is a constant four-vector.

Let us assume that the condition

$$F_q = \frac{T \operatorname{Im} G^s_{0q}}{s\, |G_{0q}|^2 (p \cdot q)} = \frac{T \gamma_k}{(p \cdot q)} \tag{22}$$

is satisfied, indicating that the "environment" (the thermostat) interacting with the wave system will be in thermodynamic equilibrium at the temperature T. It then follows from (14) that

$$s(p \cdot q)\, \Phi_q = T \operatorname{Im} \Sigma^s_q. \tag{23}$$

Let us show that if (21) holds, then (23) is satisfied within each group of graphs having the given topological structure. To do this, we make use of the properties found in sec. 1 for the graphs for Φ^s_q and Σ^s_q. We consider a certain Φ^s_q graph containing N lines in the principal part; we arrange the arrows arbitrarily in it. According to rules 7, 11, it follows that among the graphs for Σ^s_q there are exactly N graphs having the same topological structure as the graph for Φ_q and differing from it in that each of the fundamental n_q' lines in the graphs for $\operatorname{Im} \Sigma_q$ will be successively replaced by a $\operatorname{Im} G_q$' line. According to rule 11, the methods of reading the graphs for Φ_q and $\operatorname{Im} \Sigma_q$ are the same, so that within each group of graphs (23) may be written in the form

$$\int U^{s_1 s_2 \ldots s_N}_{q q_1 \ldots q_N} \Big[n^{s_1}_{q_1} \ldots n^{s_N}_{q_N} - \frac{T}{(p \cdot q)\, s} \Big(\operatorname{Im} G^{s_1}_{q_1} n^{s_2}_{q_2} \ldots n^{s_N}_{q_N} + \\ + n^{s_1}_{q_1} n^{s_2}_{q_2} \ldots \operatorname{Im} G^{s_N}_{q_N} \Big) \delta(-sq + s_1 q_1 + \ldots + s_N q_N) \Big] dq_1 \ldots dq_N = 0. \tag{24}$$

Substituting (21) into (24), we see that (24) may be rewritten as

$$\int U^{s s_1 \ldots s_N}_{q q_1 \ldots q_N} n^{s_1}_{q_1} \ldots n^{s_N}_{q_N} [-s(p \cdot q) + s_1 (p \cdot q_1) + \ldots + s_N (p \cdot q_N)] \times \\ \times \delta(-sq + s_1 q_1 + \ldots + s_N q_N)\, dq_1 \ldots dq_N = 0 \tag{25}$$

and it is evidently satisfied.

In exactly the same way, it is possible to see that (21) satisfies a system of Dyson equations for n_q, G_q for the case of a four-wave interaction Hamiltonian, as well as for an interaction Hamiltonian represented by a power series in a_k^s. Equation (21) coincides with the "fluctuation-dissipation theorem," which for thermodynamic equilibrium relates the spectral density of the fluctuations to the imaginary part of the Green's function; for a situation of thermodynamic equilibrium, it permits a transition from two equations for n_q and G_q to a single equation for G_q.

It should be noted that there is a fundamental difference between the case of thermodynamic equilibrium and the general case. In the situation of thermodynamic equilibrium, averaging is carried out over a Gibbs ensemble, and the diagram technique is just an auxiliary tool making it easier to calculate the averages. In a nonequilibrium situation, however, the diagram technique is a way of obtaining the equations for the average n_q and G_q. It is essential that in (14) the correlator for the external force F_q occur in the form of a free term and that it be possible to set it equal to 0. It is natural to assume that the solution of these equations (n_q, G_q) depends continuously on F_q and remains finite for F_q = 0. In physical terms, this means that the correlators for n_q and G_q are insensitive to the action of a small random Gaussian force on the wave field. This property of the correlators corresponds to the notion of turbulence as a result of the development of all imaginable instabilities and as the most stochastic state of the wave field.

Although the procedure for obtaining the equations for n_q and G_q is formally unambiguous, these equations are actually not uniquely defined, since the series for n_q and G_q are not absolutely convergent. This follows just from the fact that the number of topologically different trees rises factorially as the number of vertices increases. These series become unique only after definition of a summation rule for them, a problem that has as yet not been solved. It may be assumed, however, that for any summation rule the first terms of the series will remain in their locations, and in this context it makes sense to restrict the discussion to the first terms of the series for n_q and G_q even for a strong nonlinearity. For a low-level nonlinearity, the series for n_q and G_q must have an asymptotic meaning, regardless of the summation rules.

3. KINETIC EQUATION FOR WAVES

On the assumption of a low-level nonlinearity, we may neglect renormalization of the vertices and keep just the first diagrams in the expression for Φ_q and Σ_q. We write the Dyson equation for $n_{k\omega}$ as

$$n_{k\omega} = \frac{\Phi_{k\omega}}{(\omega - \tilde{\omega}_k)^2 + \gamma_{k\omega}^2}. \tag{26}$$

If the width of a packet $n_{k\omega}$ with respect to the frequencies $\Delta\omega_k$ is substantially greater than $\gamma_{k\omega} \equiv \mathrm{Im}\,\Sigma_{k\omega}$, then we may neglect the dependence of $\Phi_{k\omega}$ and $\Sigma_{k\omega}$ on ω, in this expression, taking $\omega = \omega_k = \omega_k + \mathrm{Re}\,\Sigma_k$. Then following integration with respect to ω in (26), we have

$$\gamma_k n_k = \pi \Phi_k. \tag{27}$$

Continuing to assume systematically that $\Delta\omega_k \gg \gamma_k$, we may integrate with respect to the frequencies in the expressions for $\Phi_k \equiv \Phi_k$, ω_k and $\gamma_k = \gamma_k$, ω_k, taking $n_{k\omega} \sim \delta(\omega - \omega_k)$. Then

$$\gamma_k = \frac{\pi}{2}\int |V_{k;k'k''}|^2 (n_{k'} + n_{k''})\,\delta(\omega_k - \omega_{k'} - \omega_{k''}) \times \delta(\mathbf{k} - \mathbf{k}' - \mathbf{k}'')\,d^3k'd^3k'' + \pi\int |V_{k',kk''}|^2 (n_{k''} - n_{k'}) \times \delta(\omega_{k'} - \omega_k - \omega_{k''})\,\delta(\mathbf{k}' - \mathbf{k} - \mathbf{k}'')\,d^3k'd^3k''; \tag{28}$$

$$\Phi_k = \frac{1}{2}\int |V_{k,k'k''}|^2 n_{k'} n_{k''}\,\delta(\mathbf{k} - \mathbf{k}' - \mathbf{k}'') \times \delta(\omega_k - \omega_{k'} - \omega_{k''})\,dk'dk'' + \int |V_{k',kk''}|^2 n_{k'} n_{k''} \times \delta(\mathbf{k}' - \mathbf{k} - \mathbf{k}'')\,\delta(\omega_k - \omega_{k'} - \omega_{k''})\,dk'dk''. \tag{29}$$

Substituting (28) and (29) into (27), we obtain a three-wave kinetic equation. Taking a rough estimate of γ_k from (28) to be $|V|^2 n_k k^3/\Delta\omega_k$ and taking into account the fact that our conclusion is valid if $\Delta\omega_k >> \gamma_k$, we obtain one of the criteria for applicability of the kinetic equation:

$$\Delta\omega_k > V\sqrt{n_k}\, k^{3/2} \approx V\sqrt{N}, \tag{30}$$

where $N = \int n_k\, dk \approx n_k k^3$ is the level of nonlinearity in the system.

If this condition is satisfied, the equation for $n_{k\omega}$ may be reduced to an equation for the integral quantity n_k.

Calculating the first correction for a vertex as well as the correction for the real part of the Green's function, we see that they are less than the bare values by a factor of

$$\frac{\gamma_k}{\omega''_k(\Delta k)^2} \ln\left(\frac{\omega''_k(\Delta k)^2}{\gamma_k}\right). \tag{31}$$

A theory of weak turbulence is also constructed on the basis of the parameter (31). The logarithmic factor appears when we carry out integration of diverging denominators of the type $[\omega_k - \omega_{k'} - \omega(k-k')]^{-1}$, truncated by wave damping, in k-space. It is clear from (31) that for linear dispersion there is no region of weak-turbulence applicability, and the kinetic equation cannot be used whatever the nonlinearity levels. This is easily ascertained, for example, by direct analysis of the diagram

 ,

which has no small parameter with respect to the diagram

owing to the coincidence of singularities.

4. KOLMOGOROV TURBULENT SPECTRA

In many physical problems, the quantities ω_k and $V_{kk'k''}$ are homogeneous functions of their arguments:

$$\omega_{\lambda k} = \lambda^\alpha \omega_k, \qquad V_{\lambda k, \lambda k', \lambda k''} = \lambda^t V_{kk'k''}. \tag{32}$$

It may be assumed that here the spectral characteristics of the wave field in a certain wave-number interval will also turn out to be homogeneous functions:

$$n_{k\omega} = \frac{1}{k^x} f\left(\frac{k}{\omega^{1/\beta}}\right), \qquad G_{k\omega} = \frac{1}{\omega^y} g\left(\frac{k}{\omega^{1/\beta}}\right). \tag{33}$$

The numbers x, y, β characterizing the degrees of homogeneity have come to be called scaling indices. The problem arises of the conditions for realization of the scale-invariant spectrum (33) and the determination of the scaling indices.

The problem of "scaling" turbulent spectra is associated with the name of A. N. Kolmogorov, who in 1944 suggested that the turbulence spectrum of an ideal incompressible fluid is determined by a unique quantity — the energy flux in the region of high wave numbers [7]. No rigorous proof has as yet been given for the Kolmogorov hypothesis, although many experiments aimed at measuring turbulent spectra have confirmed it with good accuracy [8]. In 1965-1966, one of the present authors developed a theory of Kolmogorov-type spectra for weak turbulence described by the kinetic equation for waves [9-12]. In this case, it was possible to find the condition for existence of Kolmogorov spectra and to demonstrate that they are exact solutions of the kinetic equations in the isotropic situation. In this case, it was found [12] that spectra with a constant flux of quasiparticles play no less important a role than do spectra with a constant energy flux; in principle, there can also be anisotropic spectra characterized by a constant momentum flux. These results were obtained with the aid of a special conformal (quasiconformal, in the more general phase) transformation in k-space. In this section, we shall apply this conformal-transformation method to the strong-turbulence case. The last decade has seen vigorous development of the theory of scale-invariant spectra in phase-transition theory; in particular, a result of the development of this theory was the establishment of the fact that indices computed with the aid of purely dimensional estimates are unreliable in most cases. This is connected with the fact that the diagrams are usually divergent for scale-invariant spectra. Thus, we shall confine the discussion to the case in which there are no such divergences or they are unimportant.

Let the system Hamiltonian have the form (2), so that $\omega_k \equiv 0$ and $V_{kk'k''}$ is a homogeneous function of degree t. Then from the equation of motion (5) we obtain an estimate interrelating the characteristic values a, k and τ (the interaction time):

$$\frac{1}{\tau} = Vak^3. \tag{34}$$

Assuming that the sole external dimensioned quantity is the flux p, we find

$$\frac{Hk^3}{\tau} \approx \frac{Va^3k^9}{\tau} \approx p \tag{35}$$

from the condition for conservation of flux. It follows from (34), (35) that

$$\frac{1}{\tau} \sim p^{1/4}V^{1/2} \sim p^{1/4}k^{t/2}, \qquad \beta = \frac{t}{2}. \tag{36}$$

We then have

$$\int n_k \omega \, d\omega \sim k^3 a_k^2 \sim \frac{1}{k^{x-\beta}} \sim \frac{p^{1/2}}{Vk^3} \sim \frac{p^{1/2}}{k^{t+3}},$$

i.e.,

$$x = t + \beta + 3 = \frac{3}{2}t + 3. \tag{37}$$

Similarly, for a four-wave Hamiltonian (18) we find

$$\beta = t/3, \qquad x = \beta + 3 + \frac{2t}{3} = t + 3. \tag{38}$$

It is then clear that for our case y = 1 for both three-wave and four-wave interaction. Despite the obvious physical interpretation of the Kolmogorov-type scale-invariant spectra found, it is not a trivial matter even for the most simple case in which all diagrams converge to verify that these solutions satisfy the diagram equations (for $n_{k\omega}$, $G_{k\omega}$).

Let us show that (36)-(38) may be obtained as a necessary condition for the solvability of the equation for $n_{k\omega}$ with a specified $G_{k\omega}$, and that in this sense the formulas (37), (38) for determination of x represent a "weak" analog of the fluctuation-dissipation theorem.

We carry out partial summation in the equations for $n_{k\omega}$ and $G_{k\omega}$ and represent the graphs for the compact parts in the form

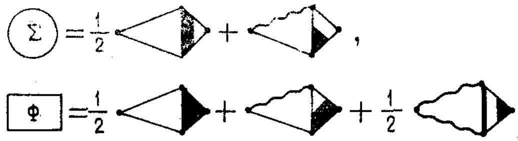

(39)

These diagrams include triple correlation functions — the vertices

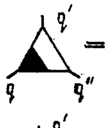 $= \dfrac{\langle a_q^{-s} f_{q'}^{-s'} f_{q''}^{-s''} \rangle}{F_{q'} F_{q''}} = \left\langle \dfrac{\delta^2 a_q^{-s}}{\delta f_{q'}^{s'} \delta f_{q''}^{s''}} \right\rangle = A_{q|q'q''}^{ss's''} \delta(sq + s'q' + s''q'')(G_q^s G_{q'}^{s'} G_{q''}^{s''}),$

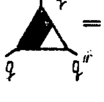 $= \dfrac{\langle a_q^{-s} a_{q'}^{-s'} f_{q''}^{-s''} \rangle}{F_{q'}} = \left\langle \dfrac{\delta a_q^{-s} a_{q'}^{-s'}}{\delta f_{q''}^{s''}} \right\rangle = B_{qq'}^{ss'}\big|_{q''}^{s''} \delta(sq + s'q' + s''q'')(G_q^s G_{q'}^{s'} G_{q''}^{s''}),$

 $= \langle a_q^{-s} a_{q'}^{-s'} a_{q''}^{-s''} \rangle = C_{qq'q''}^{ss's''} \delta(sq + s'q' + s''q'')(G_q^s G_{q'}^{s'} G_{q''}^{s''}).$ (39a)

The diagrams for the A-quadratic response is a tree having two isolated branches:

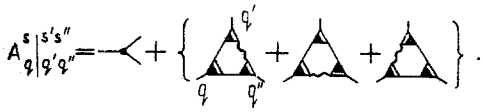

(40)

Vertex B is obtained by splicing two trees; here one branch, the output, is fixed:

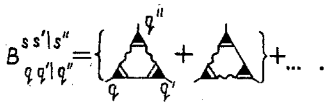

(41)

The triple correlator C appears when three trees are spliced:

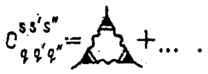

(42)

Relationships (39) have a purely topological meaning and may also be established in the noncanonical technique (see [10], for example).

Under the convergence condition for the integrals in the diagrams (40)-(42), there is coincidence of the degree of homogeneity of the renormalized vertex with the degree of the bare vertex ($t_A = t$). For this case, we have

$$t_B = t + \beta - x,$$
$$t_C = t + \alpha(\beta - x) \tag{43}$$

from (42) and (41) for the degrees t_B and t_C of the correlators $B_{qq'q''}$ and $C_{qq'q''}$. The relationships $t_A = t$ and (43) may also occur when there are divergences in the diagrams (40)-(42). We shall assume that these relationships are valid.

If the diagrams converge, we have the relationships

$$y = 1,$$
$$x = 2t + 3 - \beta \tag{44}$$

in the Dyson equation. The condition (44) may be termed the scaling condition. When there are divergences in the Dyson equation, condition (44) must be replaced by a different relationship that depends upon the cut scale. When the scaling relationships (43), (44) are satisfied, the solutions (33) formally satisfy the diagram equations.

We emphasize that in contrast to the bare vertex V, the renormalized vertices A, B do not possess symmetry with respect to permutations of the pairs $\binom{s}{q}$), since the input end points are explicit in them: these are the roots of trees colored black in the figures. Nonetheless, by virtue of the symmetry of the bare vertex (4) deriving from the fact that the initial equations are Hamiltonian, the graphs for Φ_q and Σ_q possess a certain additional symmetry that makes it possible to establish an additional relationship between the indices of the scale-invariant turbulence spectrum.

We define the combination

$$L_q = \sum_s s\left[\Phi_q^s G_q^{-s} + n_q^{-s}\Sigma_q^s\right] = 2i\,\mathrm{Im}\left(\Phi_q G_q^* + n_q^*\Sigma_q\right)$$

and note that the condition $L_{k\omega} = 0$ is equivalent to the Dyson equation for $n_{k\omega}$.

We further require that the quantity L_q be finite on the scale-invariant spectrum (33). A sufficient condition for this is the convergence of all integrals in the diagrams for G_q and Σ_q; it is also possible for the diagrams for G_q and Σ_q to diverge; the diverging terms are truncated in the expression for L_q, however. We introduce the quantity $L_\omega = \int L_{k,\omega}\,dk$. Then

$$L_\omega = \frac{1}{2}\sum_{ss's''} s\int dk\,dk'dk''\,d\omega\,d\omega'\delta(sq + s'q' + s''q'')\times$$

$$\times\left[V_{kk'k''}^{ss's''} A_q^{-s}\Big|_{q''q}^{-s''-s'} n_{q'} n_{q''} G_q^s + V_{kk'k''}^{ss's''} A_{q'}^{-s'}\Big|_{q''q}^{-s''-s} n_q n_{q''} G_{q'}^{s'} + V_{kk'k''}^{ss's''} A_{q''}^{-s''}\Big|_{q'q}^{-s'-s} G_{q''}^{s''} n_{q'} n_q\right] + \ldots\,. \tag{45}$$

For brevity, we shall not write the terms with vertices B and C. We perform a substitution of variables in the second terms (a conformal transformation),

$$\omega = \lambda\omega_1, \quad \omega' = \lambda\omega, \quad \omega'' = \lambda\omega_2, \quad \lambda \equiv \omega/\omega_1,$$
$$\boldsymbol{k} = \lambda^{\beta}\boldsymbol{k}_1, \quad \boldsymbol{k}' = \lambda^{\beta}\boldsymbol{k}, \quad \boldsymbol{k}'' = \lambda^{\beta}\boldsymbol{k}_2, \tag{46}$$
$$s = s_1, \quad s' = s, \quad s'' = s_2;$$

making use of the homogeneity of V and A and taking into account the symmetry property of vertex (4), we see that the second term in (45) on the scale-invariant spectrum goes over into the first with the factor $(\omega/\omega_1)^y(S_1/S)$. Carrying out a transformation in the third term, which differs from (46) by the substitution $\omega_1 \leftrightarrow \omega_2$, we find that the third term in (45) goes over to the first with the factor $(\omega/\omega_2)^y(S_2/S)$. The integral of the sum of these terms evidently vanishes if $y = -1$. This yields

$$x = \beta + 3 + t. \tag{47}$$

Carrying out the same operation with the remaining terms in Π_ω that contain functions B and C, we also arrive at (47).

Similar relationships may also be established between the indices β, x, and t for the case of a four-wave interaction Hamiltonian. In this case, we write the expressions for Φ_q and Σ_q in terms of the quadruple generalized vertices

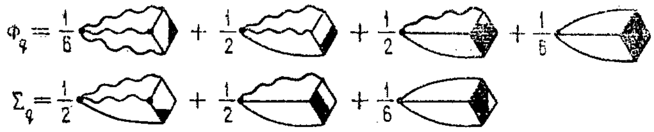

(48)

The physical meaning of these vertices becomes clear from their definition,

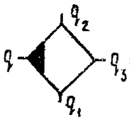

$$= \frac{\langle a_q^{-s} f_{q_1}^{-s_1} f_{q_2}^{-s_2} f_{q_3}^{-s_3} \rangle}{F_{q_1}F_{q_2}F_{q_3}} = A_q^s\Big|_{q_1q_2q_3}^{s_1s_2s_3} \delta(s_1 q + s_1q_1 + s_2q_2 + s_3q_3)\, G_q^s G_{q_1}^{s_1} G_{q_2}^{s_2} G_{q_3}^{s_3},$$

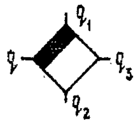

$$= B_{qq_1}^{ss_1}\Big|_{q_2q_3}^{s_2s_3} \delta(sq + s_1q_1 + s_2q_2 + s_3q_3)\, \frac{\langle a_q^{-s} a_{q_1}^{-s_1} f_{q_2}^{-s_2} f_{q_3}^{-s_3} \rangle}{F_{q_2}F_{q_3}}\, G_q^s G_{q_1}^{s_1} G_{q_2}^{s_2} G_{q_3}^{s_3}; \tag{49}$$

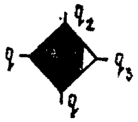

$$= C_{qq_1q_2}^{ss_1s_2}\Big|_{q_3}^{s_3} \delta(sq + s_1q_1 + s_2q_2 + s_3q_3)\, G_q^s G_{q_1}^{s_1} G_{q_2}^{s_2} G_{q_3}^{s_3}\, \frac{\langle a_q^{-s} a_{q_1}^{-s_1} a_{q_2}^{-s_2} f_{q_3}^{-s_3} \rangle}{F_{q_3}}, \tag{50}$$

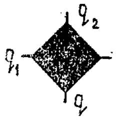

$$= D_{qq_1q_2q_3}^{ss_1s_2s_3} \delta(sq + s_1q_1 + s_2q_2 + s_3q_3)\, G_q^s G_{q_1}^{s_1} G_{q_2}^{s_2} G_{q_3}^{s_3} = \langle a_q^{-s} a_{q_1}^{-s_1} a_{q_2}^{-s_2} a_{q_3}^{-s_3} \rangle.$$

Arguing as before and assuming the compatibility of the degrees $t_A = t$, t_B, t_C, and t_D of A, B, C, and D,

$$t_B = t + \beta - x, \quad t_C = t + 2(\beta - x), \quad t_D = t + 3(\beta - x), \tag{51}$$

we obtain

$$x = \beta + 3 + \frac{2t}{3} \tag{52}$$

after application of the conformal transformation. From this and from the scaling relationship

$$x = t + 3 \tag{53}$$

we see how to verify Eqs. (38) which were previously obtained from dimensionality considerations.

Now let the Hamiltonian contain the quadratic term $\int \omega_k a_k a_k^* d\boldsymbol{k}$. There may be three cases. If the degree of homogeneity α of the frequency ω_k is great, $\alpha > \beta$, then in the region of small wave numbers the "effective dispersion" $\omega \sim \mathbf{k}^{\beta}$ due to strong turbulence exceeds the "bare dispersion" $\omega \sim \mathbf{k}^{\alpha}$, and the latter may be neglected. Here there will be weak turbulence in the region of large wave numbers. In this case, it is necessary to write $\beta = \alpha$ in (47), (52) in order to determine x, since scaling in the kinetic equation (weak scaling) imposes no conditions on the indices. The "loss" of conditions (44), (53), which are required if all terms of the series in the Dyson equations are to have the same degree of homogeneity, are essentially arbitrary, since the kinetic-equation approximation corresponds to allowance for just the first term of the series. If the random Kolmogorov relationships (47), (52) prove to be compatible with the scaling relationships (44), (53) for $\beta = \alpha$, then the nonlinear corrections to the frequency and vertex will have the degree of inhomogeneity of the corresponding bare quantities. Then as the level of nonlinearity increases, weak turbulence will continuously go over to strong turbulence. When $\alpha < \beta$, weak turbulence will occur in the region of small wave numbers, and strong turbulence will occur in the region of large numbers. We have so far spoken of Kolmogorov energy spectra.

For a four-wave Hamiltonian conserving the number of quasiparticles, $N = \int n_{\boldsymbol{k}}\, d\boldsymbol{k}$; i.e., for

$$\mathrm{H}_{\mathrm{int}} = \frac{1}{4} \int V_{12;\,34}\, a_1^* a_2^* a_3 a_4\, \delta(\boldsymbol{k}_1 + \boldsymbol{k}_2 - \boldsymbol{k}_3 - \boldsymbol{k}_4)\, d\boldsymbol{k}_1\, d\boldsymbol{k}_2\, d\boldsymbol{k}_3\, d\boldsymbol{k}_4, \tag{54}$$

there can be one more Kolmogorov particle-number spectrum. In this case, Eq. (52) has the form

$$x = 3 + 2t/3. \tag{55}$$

For an anisotropic situation there may in principle be spectra that are of Kolmogorov type with respect to the momentum: $\boldsymbol{p} = \int \boldsymbol{k}\, a_{\boldsymbol{k}} a_{\boldsymbol{k}}^* d\boldsymbol{k}$. In this case, Eq. (52) has the form

$$x = 4 + t, \tag{56}$$

and for a fourth-order Hamiltonian we have

$$x = 4 + 2t/3. \tag{57}$$

The question of which specific type of Kolmogorov spectrum we have in a particular situation is solved with an eye to the excitation conditions and other peculiarities of the problem.

At the present time, we know of no examples of actual physical media for which the integrals in all the diagrams converge to strongly turbulent Kolmogorov spectra. It must be said, however, that there is no reason in principle for this to be forbidden. Let us consider the situation for the problem of developed isotropic turbulence in an incompressible fluid.

The Euler equations for an ideal incompressible fluid do not generally permit the introduction of canonical variables. Such variables may be introduced, however, for a physically important particular class of flows for which the vortex lines take the form of lines of intersection of two families of surfaces stratifying a space. In this case, the canonical variables are introduced in accordance with the following formulas [13]:

$$\mathrm{rot}\, \boldsymbol{V} = [\nabla \lambda\, \nabla \mu], \qquad \boldsymbol{V} = \lambda \nabla \mu + \nabla \Phi \tag{58}$$

and are called the Clebsch variables. The families of surfaces spun from the vortex lines are the level surfaces of the functions $\lambda(\mathbf{r}, t)$ and $\mu(\mathbf{r}, t)$.

The variables λ, μ satisfy the equations

$$\frac{\partial \lambda}{\partial t} + (\boldsymbol{V}\nabla)\lambda = \frac{\partial \lambda}{\partial t} - \frac{\delta H}{\delta \mu} = 0, \quad \frac{\partial \mu}{\partial t} + (\boldsymbol{V}\nabla)\mu = \frac{\partial \mu}{\partial t} + \frac{\delta H}{\delta \lambda} = 0 \tag{59}$$

having the Hamiltonian

$$H = \frac{1}{2} \int V^2\, d\boldsymbol{r}. \tag{60}$$

Thus, they move together with the fluid. Single-valued Clebsch variables may be introduced if, for example, turbulence has developed owing to an instability of plane-parallel or axially symmetric laminar flow. In the general case, the variables λ, μ may be introduced locally in the neighborhood of any point, but they may prove to be multivalued functions of the coordinates.

Going over to the variables a_k, a^*_k by means of the formulas

$$\lambda_k = \frac{a_k + a^*_{-k}}{\sqrt{2}}, \qquad \mu_k = \frac{a_k - a^*_{-k}}{i\sqrt{2}},$$

we obtain the Hamiltonian of the fluid,

$$H = \frac{1}{4}\int W_{kk_1,k_2k_3}\, a^*_k\, a^*_{k_1}\, a_{k_2}\, a_{k_3}\, \delta(\boldsymbol{k}+\boldsymbol{k}_1-\boldsymbol{k}_2-\boldsymbol{k}_3)\, d\boldsymbol{k}_1\, d\boldsymbol{k}\, d\boldsymbol{k}_2\, d\boldsymbol{k}_3, \tag{60a}$$

where

$$W_{12,34} = (\varphi_{13}\varphi_{24} + \varphi_{14}\varphi_{23}), \qquad \varphi_{\alpha\beta} = \frac{1}{2}\frac{1}{(2\pi)^{3/2}}\left[\boldsymbol{k}_\alpha + \boldsymbol{k}_\beta - (\boldsymbol{k}_\alpha - \boldsymbol{k}_\beta)\frac{\boldsymbol{k}^2_\alpha - \boldsymbol{k}^2_\beta}{|\boldsymbol{k}_\alpha - \boldsymbol{k}_\beta|^2}\right].$$

Thus, the degree of homogeneity of the bare vertex is t = 2.

Equations (52) and (53) yield the familiar Kolmogorov relationship $\beta = 2/3$ determining the dependence of the characteristic time of motion of the scale. For the spectral functions $n_{k\omega}$, $G_{k\omega}$, we have

$$n_{k\omega} = \frac{1}{k^{5/3}} f\left(\frac{k}{\omega^{3/2}}\right), \qquad G_{k\omega} = \frac{1}{\omega} g\left(\frac{k}{\omega^{3/2}}\right). \tag{61}$$

Since

$$V_k = -i\int a_{k'}\, a^*_{k''}\, \varphi_{k'k''}\, \delta(\boldsymbol{k}' - \boldsymbol{k}'' - \boldsymbol{k}),$$

it is easy to express the correlation function of the velocity $I_{k\omega}$, determined by the formula

$$I_{k\omega}\, \delta(\boldsymbol{k} - \boldsymbol{k}')\, \delta(\omega - \omega') = \langle V_{k\omega} V^*_{k'\omega'} \rangle,$$

in terms of a fourth-order correlation function — the vertex $D_{12,34}$ — in accordance with (50):

$$I_q = 2\int W_{12,34}\, D^{++--}_{12,34}\, \delta(q_1 - q_4 - q)\, \delta(q_2 - q_3 - q)\, dq_1 dq_2 dq_3 dq_4. \tag{62}$$

Making use of (51) for the vertex index t_D, we find

$$I_{k\omega} \sim \frac{1}{k^{13/3}} J\left(\frac{k}{\omega^{3/2}}\right), \tag{63}$$

which for $I_k = \int I_{k\omega}\, d\omega$ corresponds to the Kolmogorov spectrum $I_k \sim 1/k^{11/3}$. This cannot be assumed to be a validated result, unfortunately. Evaluation of elementary diagrams using the Kolmogorovians $n_{k\omega}$ and $G_{k\omega}$ in the form (62) leads to divergences. For sharply noncoinciding k, the bare vertex function $W_{k_1k_2k_3k_4}$ behaves as

$$W_{k_1k_2k_3k_4} \sim |\boldsymbol{k}_1|\,|\boldsymbol{k}_2| \tag{64}$$

for $|\mathbf{k}_1|$, $|\mathbf{k}_3| \ll |\mathbf{k}_2|$, $|\mathbf{k}_4|$. Thus, the elementary diagram

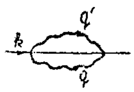

diverges as $k_0^{-2/3}$ for q, q', where k_0 is the lower boundary of the cut for integration with respect to q. Moreover, this same diagram diverges as ln k_{max}, where k_{max} is the upper boundary of the cut. The diagrams for $n_{k\omega}$ exhibit the same divergence for small q. There are also logarithmic divergences at large q in the diagrams for renormalization of the vertex parts. The scale-invariant theory of turbulence must be constructed with allowance for all these divergences.

LITERATURE CITED

1. H. W. Wyld, Ann. Phys., 14, 143 (1961).
2. L. V. Keldysh, Zh. Éksp. Teor. Fiz., 47, 1513 (1964).
3. V. I. Tatarskii, Wave Propagation in Turbulent Atmospheres [in Russian], Izd. Nauka, Moscow (1967).

4. G. A. Kuz'min and A. Z. Patashinskii, Zh. Éksp. Teor. Fiz., 62, No. 3 (1972).
5. V. E. Zakharov, Izv. Vyssh. Uchebn. Zaved., Radiofiz., 17, No. 3, 431 (1974).
6. R. E. Cutkosky, J. Math. Phys., 1, 429 (1960).
7. A. N. Kolmogorov, Dokl. Akad. Nauk SSSR, 30, No. 4, 299 (1941).
8. A. S. Monin and A. M. Yaglom, Statistical Fluid Mechanics [in Russian], Vol. 2, Izd. Nauka, Moscow (1967).
9. V. E. Zakharov, Zh. Prikl. Mekh. Tekh. Fiz., No. 4, 35 (1965).
10. V. E. Zakharov and N. N. Filonenko, Dokl. Akad. Nauk SSSR, No. 6, 1291 (1966).
11. V. E. Zakharov, Zh. Éksp. Teor. Fiz., 51, No. 8, 688 (1966).
12. V. E. Zakharov, Zh. Éksp. Teor. Fiz., 63, No. 5, 1575 (1972).
13. H. Lamb, Hydromechanics, Dover (1932).